Metal–Organic Frameworks

International Edition: DOI: 10.1002/anie.201801122
German Edition: DOI: 10.1002/ange.201801122

A Stable Metal–Organic Framework Featuring a Local Buffer Environment for Carbon Dioxide Fixation

Hongming He, Qi Sun, Wenyang Gao, Jason A. Perman, Fuxing Sun, Guangshan Zhu, Briana Aguila, Katherine Forrest, Brian Space, and Shengqian Ma**

Abstract: *A majority of metal–organic frameworks (MOFs) fail to preserve their physical and chemical properties after exposure to acidic, neutral, or alkaline aqueous solutions, therefore limiting their practical applications in many areas. The strategy demonstrated herein is the design and synthesis of an organic ligand that behaves as a buffer to drastically boost the aqueous stability of a porous MOF (JUC-1000), which maintains its structural integrity at low and high pH values. The local buffer environment resulting from the weak acid–base pairs of the custom-designed organic ligand also greatly facilitates the performance of JUC-1000 in the chemical fixation of carbon dioxide under ambient conditions, outperforming a series of benchmark catalysts.*

Metal–organic frameworks (MOFs) have received tremendous interest during the past decades owing to their designable structures and diverse physical and chemical properties useful in different applications.[1] Nonetheless, water or acidic/alkaline aqueous solutions remain a major barrier impeding MOFs in many practical areas because of damage to their pristine structures when encountering various environmental or industrial conditions.[2] Recently, various strategies for boosting MOF water stability have been explored to enhance the metal–ligand bonds and/or shield the inorganic cluster from water exposure.[3] Notwithstanding, it is also highly desirable to develop and investigate different paths to generate aqueous stable MOFs particularly under a wide range of pH conditions.

Inspired by molecules that restrict changes to pH in a buffered solution after additions of an acid or base, we postulate that MOFs containing both acidic and basic functional groups, as buffer guards, can significantly boost their stability in the presence of acidic/alkaline aqueous media. Herein, we describe an approach to construct a porous MOF that is stable over a broad pH range via employing a buffer strategy. As shown in Scheme 1, the metal–ligand bonds in the

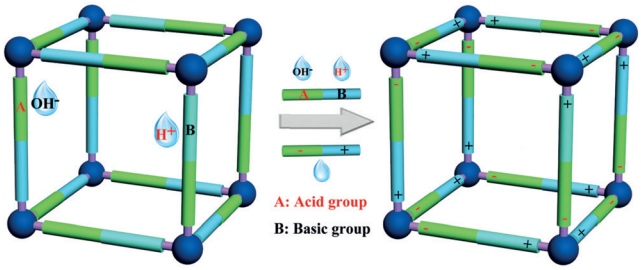

Scheme 1. Illustration of the buffer strategy in a MOF.

porous framework are susceptible to break in the presence of acid or alkaline aqueous solutions owing to the ligand deprotonation. To prevent breaking bonds, both acidic and basic functional groups can be incorporated in the MOF to participate as buffer guards to prevent assault from the acidic and alkaline media. It is anticipated that this approach will make MOFs useful for processes where water at different pH values is unavoidable.

To demonstrate this proof-of-concept, we designed and synthesized a ligand, 2,4-bis(3,5-dicarboxyphenylamino)-6-ol triazine (H_4BDPO), to behave as a buffer in which the phenol group is a weak acid with the amino and triazine groups serving as weak bases. To gain further insight into the buffer effect, a computational study was performed on a model of the buffer ligand allowing ACS/Labs software to calculate the acid dissociation constants (Supporting Information, Figures S1 and S2). The calculated p*K*a values for the functional groups are 9.4 ± 0.8 and 3.2 ± 0.8 for the acid (aromatic N, −NH−) and base (−OH), respectively. Furthermore, the maximum buffer capacity is in the pH range from 1.1 to 11.9. The ligand can undergo changes in its total charge at high or low pH values due to the presence of $-O^-/-OH$, $-NH-/-NH^+-$, and $-N=/-NH^+=$ pairs (the so-called buffering effect).[4] Furthermore, the total charge depends on the ionogenic groups at different pH values, where it can change from -1 to $+1$ (Supporting Information, Figure S3 and Table S1). As such, this ligand, within a MOF, can serve as

[*] Dr. H. He, Prof. G. Zhu
Key Laboratory of Polyoxometalate Science of the Ministry of Education, College of Chemistry, Northeast Normal University
Changchun (P. R. China)
E-mail: zhugs@jlu.edu.cn
Dr. H. He, Dr. Q. Sun, Dr. W. Gao, Dr. J. A. Perman, B. Aguila, K. Forrest, Prof. B. Space, Prof. S. Ma
Department of Chemistry, University of South Florida
Tampa, FL 33620 (USA)
E-mail: sqma@usf.edu
Dr. H. He
Key Laboratory of Inorganic-Organic Hybrid Functional Material Chemistry, Ministry of Education, College of Chemistry
Tianjin Normal University, Tianjin (P. R. China)
Dr. H. He, Dr. F. Sun, Prof. G. Zhu
State Key Laboratory of Inorganic Synthesis and Preparative Chemistry, College of Chemistry, Jilin University
Changchun (P. R. China)
Supporting information and the ORCID identification number(s) for the author(s) of this article can be found under: https://doi.org/10.1002/anie.201801122.

a buffer guard to prevent assault from acidic and alkaline media.

Among various types of inorganic building blocks in MOFs, the copper paddlewheel cluster, $[Cu_2(O_2C{-})_4]$, has been ubiquitously applied to construct porous MOFs with high accessible surface areas and a high concentration of open metal sites (OMSs).[5] Therefore, we reacted the buffer molecule H_4BDPO with copper nitrate (for details, see the Supporting Information) under suitable conditions to form the copper paddlewheel cluster that led to a microporous MOF, $[Cu_{24}(BDPO)_{12}(H_2O)_{12}]\cdot 30\,DMF\cdot 14\,H_2O$ (namely JUC-1000, DMF = *N*,*N*′-dimethylformamide). The strategy in this work, as shown in Scheme 2, involves: 1) an asymmetric

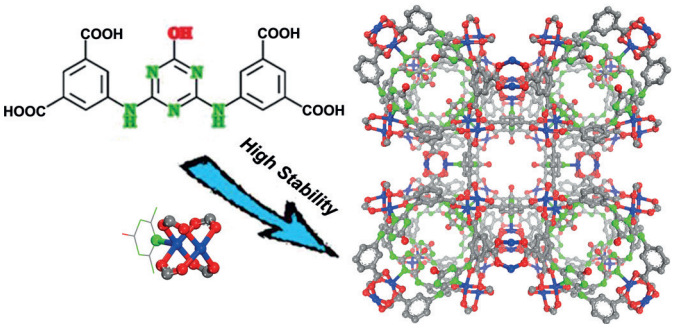

Scheme 2. Illustration of the buffer strategy for the construction of a stable MOF, JUC-1000.

copper paddlewheel where the copper atoms are 5-coordinate from four carboxylate groups (equatorial positions) and with either a nitrogen atom from the ligand triazine moiety or a water molecule (removed for clarity) in the axial position; 2) the access to the functional groups −OH, −NH−, and 1,3,5-triazine, which function as buffer sites to enhance the stability in acidic and alkaline media; and 3) dehydration on the copper paddlewheel, which will help facilitate adsorption sites allowing CO_2 transformation reactions. Remarkably, the acidic (−OH)[6] and basic (−NH−, 1,3,5-triazine)[7] functional groups played crucial roles in the CO_2 cycloaddition reaction as indicated from previous research. In this contribution, we show that JUC-1000 displays excellent water and acidic/alkaline stability. Furthermore, it exhibits exceptionable recyclable CO_2 capture and conversion performance under ambient conditions. We regard this strategy to add safeguards into the framework to enhance its stability, but also include open metal sites and functional organic groups for efficient chemical fixation of CO_2.

Single-crystal X-ray diffraction studies revealed that JUC-1000 crystallized in the cubic space group $Im\bar{3}m$ (Supporting Information, Figure S4). The ligand contains two terminal isophthalate moieties, which are assembled with copper paddlewheel motifs to fabricate the typical cuboctahedral MOP-1 (metal-organic polyhedron) (Figure 1 a).[8] Another medium cage of cuboid configuration is formed by eight $[Cu_2(O_2C{-})_4]$ units and four ligand linkers (Figure 1 b). The small octahedral cage is generated through six $[Cu_2(O_2C{-})_4]$ units and six linkers (Figure 1 c). The three types of polyhedron pack to assemble a 3D MOF with multiple pores

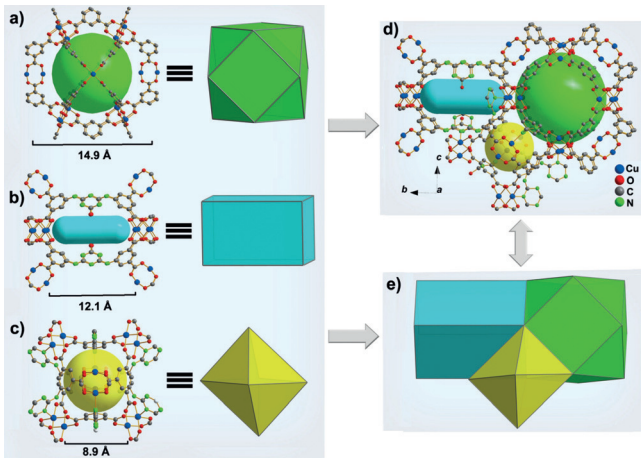

Figure 1. Crystallographic views and model representations of a) cuboctahedron, b) cuboid, c) octahedron, and d),e) their crystal packing positions.

(Figure 1 d,e; Supporting Information, Figure S5). From a topologic point of view, the resulting 3D network can be symbolized as a rare 5-connected uninodal network with the point (Schläfli) symbol $[4^6{\cdot}6^4]$ and the vertex symbol [4.4.4.4.4.4.6.6.8(4).8(4)] as calculated with TOPOS software (Supporting Information, Figure S6).[9] The total void volume in JUC-1000 was calculated to be 53.9 % after eliminating guest and coordinated water molecules using the PLATON/VOID routine.[10]

The phase purity was confirmed by powder X-ray diffraction (PXRD) studies (Supporting Information, Figure S7), which showed good agreement between the calculated and experimental patterns. The thermogravimetric analysis of the as-synthesized sample (Supporting Information, Figure S8 a) showed a weight loss of 4.9 % before 130 °C, corresponding to the loss of H_2O molecules (calculated 4.9 %). With the temperature increasing, the second weight loss is about 22.5 % from 130 °C to 300 °C, belonging to the loss of DMF molecules (calculated 22.8 %). Structural decomposition began around 350 °C. The activated sample was prepared by exchanging the reaction solvent with CH_3OH and then CH_2Cl_2 for three days, followed by evacuation under high vacuum at 150 °C for 12 h. The PXRD pattern of the activated sample matched well with the calculated one from the single crystal data, which confirmed that JUC-1000 retained its crystallinity after activation (Supporting Information, Figure S7). The intensities of some of the peaks were different between the calculated and experimental patterns, which is presumably due to the loss of solvent molecules in the MOF sample.[3d] As shown in the Supporting Information, Figures S8 b and S9, guest and terminal solvent molecules were completely removed. The permanent porosity of activated JUC-1000 was determined by N_2 sorption measurements at 77 K and showed a reversible type-I isotherm, characteristic of microporous materials, with a high N_2 uptake of 313 $cm^3\,g^{-1}$ (Figure 2). The calculated Brunauer–Emmett–Teller (BET) surface area was 1221 $m^2\,g^{-1}$ (Langmuir surface area: 1364 $m^2\,g^{-1}$). JUC-1000 was shown to possess three types of

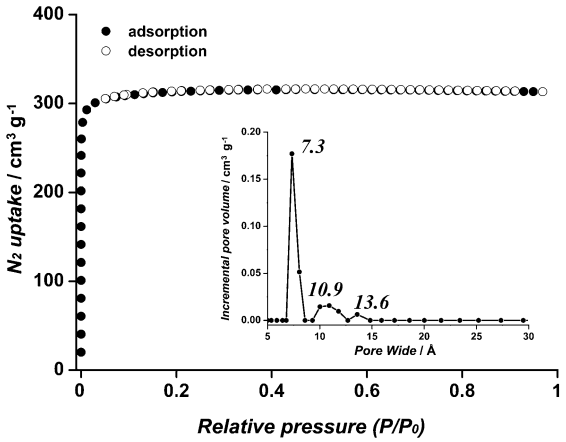

Figure 2. N_2 sorption isotherm of the activated sample at 77 K. Inset: pore size distribution calculated by the DFT method.

pores at 7.3, 10.9 and 13.6 Å, calculated using the DFT method, which agreed well with those observed from the single crystal structure. Furthermore, JUC-1000 exhibited high stability under different chemical and thermal conditions (Supporting Information, Figures S10 and S11).

Furthermore, we systematically assessed the water and acidic/alkaline stability of JUC-1000 by boiling it in water for 7 days or immersing it in pH 1.5 (HCl) and pH 12.5 (NaOH) aqueous solutions for 2 days at room temperature (Supporting Information, Figure S12). The maximum buffer capacity is in the pH range from 1.5 to 12.5, which agreed with the calculated results (pH 1.1–11.9). PXRD patterns and surface areas have been employed to evaluate the preservation of crystallinity and structural integrity for MOFs. As shown in Figure 3a,b, JUC-1000 possessed excellent water and acidic/alkaline stability. Furthermore, inductively coupled plasma optical emission spectrometry (ICP-OES) analysis (Supporting Information, Table S2) and UV/Vis spectrum studies of Cu^{II} (Supporting Information, Figure S13) were both measured to confirm there was no leaching of Cu^{II} ions into the acid or base solution. The pH values of the solution before and after addition of JUC-1000 to the solution changed from 12.5 to 11.69 in the base solution, and from 1.5 to 2.76 in the acid solution, respectively. Furthermore, the water solution with or without JUC-1000 was titrated with 0.5 M aqueous HCl or 0.2 M aqueous NaOH to measure the pH values, respectively, which further highlighted that JUC-1000 can efficiently prevent the assault from the acidic and alkaline media (Supporting Information, Figure S14). Additional control experiments were performed for HKUST-1,[11] MOF-74-(Mg),[12] UiO-66,[13] UiO-66-NO_2,[14] and ZIF-8[15] under the same conditions. HKUST-1 is a representative copper paddlewheel MOF, which was easily decomposed under these conditions (Figure 3c,d). MOF-74(Mg) was stable in boiling water, but its crystallinity was completely lost at pH 1.5 and a portion of the framework collapsed after exposure to a pH 12.5 aqueous solution (Figure 3e,f). UiO-66 treated with a pH 12.5 aqueous solution led to complete degradation of the framework (Figure 3g,h). UiO-66-NO_2 was also completely collapsed after treating with a pH 12.5 aqueous solution for 2 days (Figure 3i,j). ZIF-8 maintained crystallinity after exposure to boiling water and a pH 12.5 aqueous solution, but it was dissolved in a pH 1.5 aqueous solution (Figure 3k,l). Their surface areas are listed in Table 1 after various tests. These results further suggest that the buffering method is capable of improving the tolerance for copper paddlewheel MOFs toward water and acidic/alkaline media.

We further measured the sorption behaviors of activated JUC-1000 for some small gases (Supporting Information, Figures S15–S25). It is worth noting that CO_2 adsorption reached 125 $cm^3 g^{-1}$ and 80 $cm^3 g^{-1}$ at 273 and 298 K under 1 atm (Supporting Information, Figure S26a). The CO_2 adsorption sharply decreased with increase in temperature from 273 K to 298 K, which was mainly attributed to the

Table 1: Surface areas [$m^2 g^{-1}$] for JUC-1000, HKUST-1, MOF-74(Mg), UiO-66, UiO-66-NO_2, and ZIF-8 after various tests.[a]

Conditions	JUC-1000	HKUST-1	MOF-74(Mg)	UiO-66	UiO-66-NO_2	ZIF-8
As-synthesized	1220(87)	1648(71)	1470(01)	1118(96)	524(11)	1307(28)
Boiling water	1199(80)	ND	1482(30)	1079(35)	526(49)	1298(85)
pH 1.5 HCl(aq)	1154(50)	ND	ND	1075(06)	521(27)	D
pH 12.5 NaOH(aq)	1206(61)	ND	455(61)	116(76)	ND	1301(81)

[a] Values were obtained from N_2 sorption measurements at 77 K in different conditions. ND: not determined. D: dissolved.

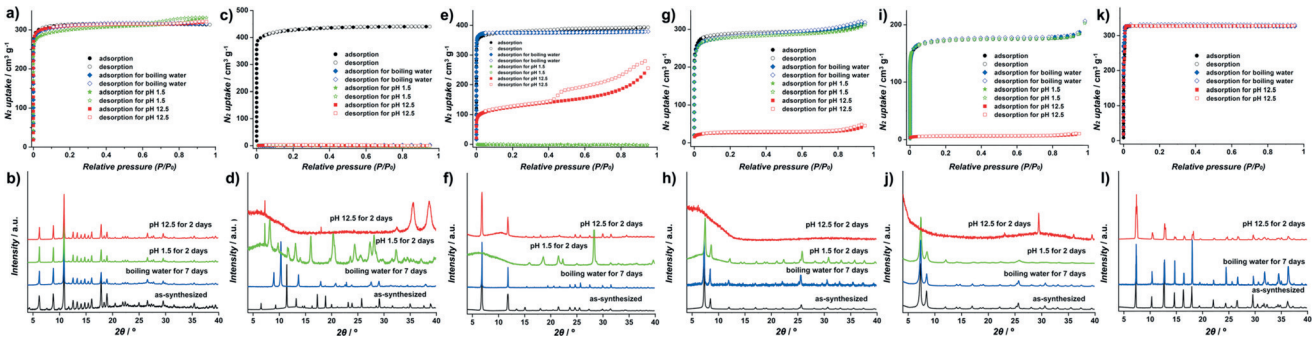

Figure 3. N_2 sorption isotherms at 77 K and PXRD patterns for a),b) JUC-1000, c),d) HKUST-1, e),f) MOF-74(Mg), g),h) UiO-66, i),j) UiO-66-NO_2, and k),l) ZIF-8 after each stability test.

relatively large pores for CO_2 and the significant increase of CO_2 thermal agitation at higher temperatures. The result is similar with aforementioned porous copper paddlewheel-MOFs with many polar groups.[16] The isosteric heat of CO_2 adsorption (Q_{st}) at zero coverage was calculated to be 23 kJ mol^{-1} (Supporting Information, Figure S26b) using the virial method.[17] Classical annealing simulations using the massively parallel Monte Carlo (MPMC)[18] code indicate primary CO_2 sorption occurs between two adjacent linkers coordinated to their hydroxide functionality (Supporting Information, Figure S27). Binding energy, determined from density functional theory calculations using the Vienna ab initio simulation package,[19–21] was calculated to be 25.2 kJ mol^{-1}, in good agreement with the Q_{st} derived from isotherms.

By virtue of the excellent stability, open metal sites, functional groups, and high CO_2 adsorption capacity of JUC-1000, we decided to investigate its catalytic performance for the cycloaddition reaction of CO_2 and epoxides to form cyclic carbonates under solvent-free conditions at room temperature and 1 atm. The percent yields were determined by ^{1}H NMR (Supporting Information, Figures S28–S39). For comparison we additionally used HKUST-1 and MOF-505 with copper paddlewheel clusters to manifest that JUC-1000 has significantly enhanced catalytic efficiency. As shown in Table 2, entry 1, the activated JUC-1000 exhibited efficient catalytic activity for the cycloaddition of propylene oxide and CO_2 to form propylene carbonate with a yield of 96%. HKUST-1 and MOF-505 showed moderate catalytic activity with propylene carbonate yields of 62% and 61% (entries 2 and 3), respectively, under similar conditions. The corresponding turnover frequency (TOF) values of JUC-1000, HKUST-1, and MOF-505 for propylene carbonate were 160, 103, and 102 h^{-1}, respectively. We reasoned that the high catalytic activity of JUC-1000 may be ascribed to the high stability and many (−OH) and (−NH−) functional groups on the ligand. Besides open Cu^{II} metal sites, the reaction can also be activated by these functional groups via forming hydrogen bonds with the oxygen atom of the epoxide ring.[18] Furthermore, the yield of cyclic carbonate drastically decreased with the increase of the epoxide substrate molecular size (entries 4, 5, and 6). The yields of cycloaddition products decreased to 81%, 58%, and 29% for butylene oxide, 1,2-epoxy-3-allyloxypropane, and benzyl phenylglycidyl ether, respectively. This phenomenon may be primarily ascribed to the slowed diffusion of large-sized substitute molecules into the framework with the increase of molecule size from $4.2\times2.6\times1.8$ Å^3 of propylene oxide to $9.4\times4.3\times2.3$ Å^3 of benzyl phenylglycidyl ether.[19] When the same reaction was performed without JUC-1000, almost no product was generated (entry 7), which indicated the significance of JUC-1000 during the catalytic process. Owing to the high stability, JUC-1000 can be recycled without any significant decrease in the catalytic performance after five cycles (entry 8). The structural integrity after catalysis was affirmed by PXRD patterns (Supporting Information, Figure S38c) and CO_2 adsorption (Supporting Information, Figure S38d) experiments. Additionally, ICP-OES analysis showed the absence of Cu^{II} from the reaction mixture thus confirming the heterogeneous nature of the reaction. Compared with other reported MOF-based heterogeneous catalysts, JUC-1000 exhibited excellent efficiency in CO_2 conversion under ambient conditions (Supporting Information, Table S4).[16a,b,20] Notably, we not only introduced a buffer proof-of-concept to enhance the stability, but also provide (−OH) and (−NH−) functional groups as hydrogen bonds to enhance the catalytic effect for the cycloaddition reaction of CO_2 and epoxides to form cyclic carbonates.

Table 2: Various carbonates from their respective epoxides catalyzed by different catalysts.

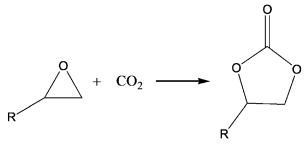

Entry	Catalyst	Epoxide	Product	Yield [%][d]
1[a]	JUC-1000			96
2[a]	HKUST-1			62
3[a]	MOF-505			61
4[a]	JUC-1000			81
5[a]	JUC-1000	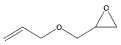	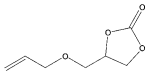	58
6[a]	JUC-1000	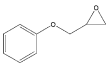	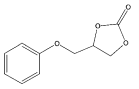	29
7[b]	–			3
8[c]	JUC-1000			96

[a] Reaction conditions: epoxide (20.0 mmol) with catalyst (0.25 mol% per exposed copper site), TBABr (0.65 g), at room temperature under 1 atm CO_2 for 48 hours. [b] The same reaction conditions as in [a], but without the catalyst. [c] The recyclability test, after five cycles. [d] The percentage yields were determined by ^{1}H NMR spectroscopy.

Based on the crystal structure, we proposed an assumptive mechanism for the chemical fixation reaction of CO_2 catalyzed by JUC-1000 (Supporting Information, Figure S40).[22–24] The overall process involves four major steps. The reaction is initiated by activation of the epoxide ring, which is synergistically facilitated by the oxygen atom of the epoxide ring coordinating with the open Cu^{II} Lewis site and also forming hydrogen bonds with the (−OH) and (−NH−) functional groups on the ligand. Subsequently, the epoxide rings are opened by Br^- from TBABr, which can attack the less-hindered carbon atoms of both the coordinated and hydrogen-bonded epoxides. The resultant intermediate oxygen anions from the opened epoxy rings then rapidly

react with the surrounding CO_2 molecules, which have been attracted and activated by Lewis basic sites (−NH− and 1,3,5-triazine) within the porous framework, to generate alkycarbonate anions. The transformation of alkycarbonate anions into the corresponding cyclic carbonates is achieved through the cyclization step. Hence, it is can be inferred that the overall process of chemical fixation of CO_2 can be significantly promoted by the incorporation of weak acidic and basic functional groups within the MOF; although detailed mechanistic studies to identify the intermediates during this process are needed, this is beyond the scope of this work and will be conducted in the near future.

In summary, we demonstrated a buffer strategy to drastically boost the water and chemical stability of MOFs as exemplified by constructing a stable copper paddlewheel based MOF (JUC-1000) using a custom-designed buffer behaving ligand that features both weak acidic and basic functional groups. Benefiting from the weak acid–base pairs that facilitate both the activation and interactions of epoxide and CO_2 molecules, the MOF, JUC-1000, exhibited excellent performance in the chemical fixation of carbon dioxide to form fine chemicals under ambient conditions. This buffer strategy demonstrates unique advantages over existing MOFs and can be further extended to a wide range of applications that require moisture and acidic/alkaline media stability.

Acknowledgements

We are grateful for the financial support of the Tianjin Science and Technology Fund Project for High Education (2017KJ127), Doctoral Program Foundation of Tianjin Normal University (043135202-XB1702), National Basic Research Program of China (973 Program, grant no. 2012CB821700 and 2014CB931804), Major International (Regional) Joint Research project of NSFC (grant no. 21120102034), NSFC Project (grant no. 21531003), NSF (DMR-1352065), and USF for financial support of this work. Computational resources were made available by a XSEDE Grant (No. TG-DMR090028) and by Research Computing at the University of South Florida.

Conflict of interest

The authors declare no conflict of interest.

Keywords: acid–base pairs · buffers · carbon dioxide fixation · metal–organic frameworks · stability

How to cite: *Angew. Chem. Int. Ed.* **2018**, *57*, 4657–4662
Angew. Chem. **2018**, *130*, 4747–4752

[1] a) H.-C. Zhou, J. R. Long, O. M. Yaghi, *Chem. Rev.* **2012**, *112*, 673–674; b) H.-C. Zhou, S. Kitagawa, *Chem. Soc. Rev.* **2014**, *43*, 5415–5418; c) J. Jiang, Y. Zhao, O. M. Yaghi, *J. Am. Chem. Soc.* **2016**, *138*, 3255–3265; d) S. M. Cohen, *Chem. Rev.* **2012**, *112*, 970–1000; e) B. Li, M. Chrzanowski, Y. Zhang, S. Ma, *Coord. Chem. Rev.* **2016**, *307*, 106–129.

[2] a) N. C. Burtch, H. Jasuja, K. S. Walton, *Chem. Rev.* **2014**, *114*, 10575–10612; b) J. A. Greathouse, M. D. Allendorf, *J. Am. Chem. Soc.* **2006**, *128*, 10678–10679; c) T. Li, D.-L. Chen, J. E. Sullivan, M. T. Kozlowski, J. K. Johnson, N. L. Rosi, *Chem. Sci.* **2013**, *4*, 1746–1755; d) J. M. Taylor, R. Vaidhyanathan, S. S. Iremonger, G. K. H. Shimizu, *J. Am. Chem. Soc.* **2012**, *134*, 14338–14340.

[3] a) W. Zhang, Y. Hu, J. Ge, H.-L. Jiang, S.-H. Yu, *J. Am. Chem. Soc.* **2014**, *136*, 16978–16981; b) T. Wu, L. Shen, M. Luebbers, C. Hu, Q. Chen, Z. Ni, R. I. Masel, *Chem. Commun.* **2010**, *46*, 6120–6122; c) J. G. Nguyen, S. M. Cohen, *J. Am. Chem. Soc.* **2010**, *132*, 4560–4561; d) W.-Y. Gao, R. Cai, T. Pham, K. A. Forrest, A. Hogan, P. Nugent, K. Williams, L. Wojtas, R. Luebke, L. J. Weselinski, M. J. Zaworotko, B. Space, Y.-S. Chen, M. Eddaousi, X. Shi, S. Ma, *Chem. Mater.* **2015**, *27*, 2144–2151; e) Q. Sun, H. He, W.-Y. Gao, B. Aguila, L. Wojtas, Z. Dai, J. Li, Y.-S. Chen, F.-S. Xiao, S. Ma, *Nat. Commun.* **2016**, *7*, 13300; f) K. Wang, X.-L. Lv, D. Feng, J. Li, S. Chen, J. Sun, L. Song, Y. Xie, J.-R. Li, H.-C. Zhou, *J. Am. Chem. Soc.* **2016**, *138*, 914–919; g) Y. Sun, Q. Sun, H. Huang, B. Aguila, Z. Niu, J. A. Perman, S. Ma, *J. Mater. Chem. A* **2017**, *5*, 18770–18776; h) Y.-X. Tan, Y. Si, W. Wang, D. Yuan, *J. Mater. Chem. A* **2017**, *5*, 23276–23282; i) L. Liang, C. Liu, F. Jiang, Q. Chen, L. Zhang, H. Xue, H.-L. Jiang, J. Qian, D. Yuan, M. Hong, *Nat. Commun.* **2017**, *8*, 1233–1242; j) A. J. Howarth, Y. Liu, P. Li, Z. Li, T. C. Wang, J. T. Hupp, O. K. Farha, *Nat. Mater. Rev.* **2016**, *1*, 15018–15032.

[4] a) J. Li, Z. Jiang, H. Wu, L. Zhang, L. Long, Y. Jiang, *Soft Matter* **2010**, *6*, 542–550; b) S. H. Zhang, Z. Y. Jiang, X. L. Wang, C. Yang, J. F. Shi, *ACS Appl. Mater. Interfaces* **2015**, *7*, 19570–19578.

[5] a) F. Nouar, J. F. Eubank, T. Bousquet, L. Wojtas, M. J. Zaworotko, M. Eddaoudi, *J. Am. Chem. Soc.* **2008**, *130*, 1833–1835; b) S. S.-Y. Chui, S. M.-F. Lo, J. P. H. Charmant, A. G. Orpen, I. D. Williams, *Science* **1999**, *283*, 1148–1150; c) B. Li, H.-M. Wen, H. Wang, H. Wu, M. Tyagi, T. Yildirim, W. Zhou, B. Chen, *J. Am. Chem. Soc.* **2014**, *136*, 6207–6210.

[6] a) L. Han, H. Li, S.-J. Choi, M.-S. Park, S.-M. Lee, Y.-J. Kim, D.-W. Park, *Appl. Catal. A* **2012**, *429–430*, 67–72; b) R. Luo, X. Zhou, Y. Fang, H. Ji, *Carbon* **2015**, *82*, 1–11; c) J. Sun, S. Zhang, W. Cheng, J. Ren, *Tetrahedron Lett.* **2008**, *49*, 3588–3591.

[7] a) S.-D. Lee, B.-M. Kim, D.-W. Kim, M.-I. Kim, K. R. Roshan, M.-K. Kim, Y.-S. Won, D.-W. Park, *Appl. Catal. A* **2014**, *486*, 69–76; b) Z.-Z. Yang, L.-N. He, C.-X. Miao, S. Chanfreau, *Adv. Synth. Catal.* **2010**, *352*, 2233–2240; c) Y.-M. Shen, W.-L. Duan, M. Shi, *Eur. J. Org. Chem.* **2004**, 3080–3089; d) Y.-H. Han, Z.-Y. Zhou, C.-B. Tian, S.-W. Du, *Green Chem.* **2016**, *18*, 4086–4091.

[8] M. Eddaoudi, J. Kim, J. B. Wachter, H. K. Chae, M. O'Keeffe, O. M. Yaghi, *J. Am. Chem. Soc.* **2001**, *123*, 4368–4369.

[9] V. A. Blatov, *IUCr CompComm Newsletter* **2006**, *7*, 4–38; see also http://www.topos.ssu.samara.ru.

[10] A. L. Spek, *J. Appl. Crystallogr.* **2003**, *36*, 7–13.

[11] N. C. Jeong, B. Samanta, C. Y. Lee, O. K. Farha, J. T. Hupp, *J. Am. Chem. Soc.* **2012**, *134*, 51–54.

[12] P. D. C. Dietzel, R. Blom, H. Fjellvag, *Eur. J. Inorg. Chem.* **2008**, 3624–3632.

[13] J. H. Cavka, S. Jakobsen, U. Olsbye, N. Guillou, C. Lamberti, S. Bordiga, K. P. Lillerud, *J. Am. Chem. Soc.* **2008**, *130*, 13850–13851.

[14] a) M. Kandiah, M. H. Nilsen, S. Usseglio, S. Jakobsen, U. Olsbye, M. Tilset, C. Larabi, E. A. Quadrelli, F. Bonino, K. P. Lillerud, *Chem. Mater.* **2010**, *22*, 6632–6640; b) C. Xiao, T. W. Goh, K. Brashler, Y. Pei, Z. Guo, W. Huang, *J. Phys. Chem. B* **2014**, *118*, 14168–14176.

[15] K. S. Park, Z. Ni, A. P. Cote, J. Y. Choi, R. Huang, F. Uribe-Romo, H. K. Chae, M. O'Keeffe, O. M. Yaghi, *Proc. Natl. Acad. Sci. USA* **2006**, *103*, 10186–10191.

[16] a) P.-Z. Li, X.-J. Wang, J. Liu, J. S. Lim, R. Zou, Y. Zhao, *J. Am. Chem. Soc.* **2016**, *138*, 2142 – 2145; b) P.-Z. Li, X.-J. Wang, J. Liu, H. S. Phang, Y. Li, Y. Zhao, *Chem. Mater.* **2017**, *29*, 9256 – 9261; c) J. Park, J.-R. Li, Y.-P. Chen, J. Yu, A. A. Yakovenko, Z. U. Wang, L.-B. Sun, P. B. Balbuena, H.-C. Zhou, *Chem. Commun.* **2012**, *48*, 9995 – 9997.
[17] L. Czepirski, J. Jagiello, *Chem. Eng. Sci.* **1989**, *44*, 797 – 801.
[18] J. L. Belof, B. Space, Massively Parallel Monte Carlo (MPMC). Available on GitHub, **2012**; https://github.com/mpmccode/mpmc.
[19] G. Kresse, J. Hafner, *Phys. Rev. B* **1993**, *47*, 558 – 561.
[20] G. Kresse, J. Hafner, *Phys. Rev. B* **1994**, *49*, 14251 – 14269.
[21] G. Kresse, J. Furthmuller, *Comput. Mater. Sci.* **1996**, *6*, 15 – 50.
[22] a) D. Ji, X. Lu, R. He, *Appl. Catal. A* **2000**, *203*, 329 – 333; b) M. Tu, R. J. Davis, *J. Catal.* **2001**, *199*, 85 – 91; c) M. H. Beyzavi, R. C. Klet, S. Tussupbayev, J. Borycz, N. A. Vermeulen, C. J. Cramer, J. F. Stoddart, J. T. Hupp, O. K. Farha, *J. Am. Chem. Soc.* **2014**, *136*, 15861 – 15864.
[23] Z. Zhou, C. He, J. Xiu, L. Yang, C. Duan, *J. Am. Chem. Soc.* **2015**, *137*, 15066 – 15069.
[24] a) W.-Y. Gao, Y. Chen, Y. Niu, K. Williams, L. Cash, P. J. Perez, L. Wojtas, J. Cai, Y.-S. Chen, S. Ma, *Angew. Chem. Int. Ed.* **2014**, *53*, 2615 – 2619; *Angew. Chem.* **2014**, *126*, 2653 – 2657; b) W.-Y. Gao, L. Wojtas, S. Ma, *Chem. Commun.* **2014**, *50*, 5316 – 5318; c) S. Kumar, G. Verma, W.-Y. Gao, Z. Niu, L. Wojtas, S. Ma, *Eur. J. Inorg. Chem.* **2016**, 4373 – 4377; d) Z. R. Jiang, H. Wang, Y. Hu, J. Lu, H. L. Jiang, *ChemSusChem* **2015**, *8*, 878 – 885; e) W.-Y. Gao, C. Y. Tsai, L. Wojtas, T. Thiounn, C. C. Lin, S. Ma, *Inorg. Chem.* **2016**, *55*, 7291 – 7294; f) H. He, J. A. Perman, G. Zhu, S. Ma, *Small* **2016**, *12*, 6309 – 6324; g) X. Wang, W.-Y. Gao, Z. Niu, L. Wojtas, J. A. Perman, Y.-S. Chen, Z. Li, B. Aguila, S. Ma, *Chem. Commun.* **2018**, *54*, 1170 – 1173.

Manuscript received: January 26, 2018
Revised manuscript received: February 17, 2018
Accepted manuscript online: February 19, 2018
Version of record online: March 15, 2018

